

Detection of Biomolecules on Surfaces Using Ion-Beam-Induced Desorption and Multiphoton Resonance Ionization

D. M. Hrubowchak, M. H. Ervin, M. C. Wood, and Nicholas Winograd*

Department of Chemistry, 152 Davey Laboratory, The Pennsylvania State University, University Park, Pennsylvania 16802

Multiphoton resonance ionization (MPRI) has been combined with ion-beam-induced desorption to examine a set of thermally labile biological molecules present on surfaces. Specifically, we have examined films of adenine and β -estradiol, molecules with a rigid skeletal backbone. In both of these cases, molecular ions could be produced efficiently without cooling the neutral molecules into their ground vibrational state. We have also studied other more fragile molecules such as tryptamine, tryptophan, phenylalanine, and serotonin. The base peak in the mass spectra of these molecules is fragment ions formed by losses of the amine side chains. Even with this fragmentation, however, it is possible to achieve sensitivity limits that are many orders of magnitude greater than for secondary ion mass spectrometry, without preparing the samples in special matrices. For serotonin, detection limits of 40 fmol on the surface of a silicon target are achievable. The results also yield a linear relation between the serotonin base fragment ion intensity and the known surface concentration.

INTRODUCTION

Multiphoton resonance ionization (MPRI) has been successfully utilized as a means of detecting neutral atoms and molecules desorbed from surfaces using kiloelectronvolt ion beams (1-6). For atoms, this approach provides unprecedented selectivity and subattomole sensitivity for surface analysis (3). These limits are possible to achieve because each analyte has a finite number of accessible excited states that also exhibit large photon absorption cross sections which permit efficient photoionization. For molecules, subfemtomole detection limits have been reported for some cases, although the degree of selectivity is greatly reduced (4). The analytical procedure is not as straightforward as for atoms since there is nearly a continuum of energy levels accessible to laser excitation and since target molecules may be fragmented either during the desorption event or during the photoionization event (7). Early results, however, demonstrate significant improvements over secondary ion mass spectrometry (SIMS) both in sensitivity and in quantitation (4).

With this measurement scheme, a pulsed beam of kiloelectronvolt noble gas ions is focused onto the sample. During

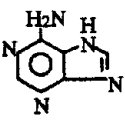
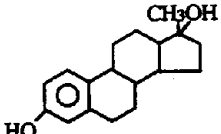
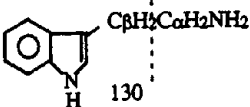
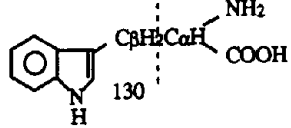
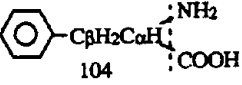
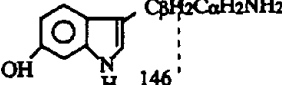
the ion impact event, sufficient momentum is transferred to the target molecules to induce desorption from surface layers. These gas-phase molecules are produced in a variety of rotational, vibrational, and electronic excited states. A small fraction may even be ionized. After a time delay, a high-power tunable pulsed laser is used to interrogate this plume of desorbed molecules, producing photoions. These ions are then characterized by using time-of-flight (TOF) mass spectrometry.

There are several important criteria for choosing the photoionization wavelength. First, the molecular species must absorb in a wavelength regime that is accessible to the laser system. Aromatic molecules are particularly suitable in this regard since they absorb strongly in the near ultraviolet (UV). Second, the wavelength must be of sufficient energy to excite the molecule to the first excited state ($S_1 \leftarrow S_0$). Moreover, when two photons are absorbed, the energy sum must exceed the ionization potential of the molecule.

We have recently found that the MPRI method is an effective means of characterizing monolayers of organic molecules with subfemtomole sensitivity (4). Intense molecular ion signals have been observed in the TOF mass spectra of several polycyclic aromatic compounds (PAC's) desorbed from both insulating and conducting surfaces. These compounds are well-suited for MPRI detection in the sense that they possess many internal degrees of freedom that can soak up a relatively large amount of energy that is deposited into the molecule by the desorption and photoionization processes. Moreover, the PAC's investigated in these studies do not have any alkyl side chains attached that may present potential fragmentation pathways.

In this paper, we show that the MPRI approach is well-suited to probing the neutral flux of a variety of structurally fragile target molecules. Specifically, we have examined the response of ion-bombarded surfaces containing aromatic compounds with amine or amino acid side chains and aromatic systems with heteroatoms as well as compounds with a significant degree of nonaromatic character. Each molecule displays biogenic activity and is of pharmaceutical and medical interest. The results show that intense molecular ions are observed for all the molecules without side chains. For other types of molecules, it is more difficult to obtain unfragmented molecular ions. Structurally specific fragments generally form the base peak in the TOF mass spectra. This fragmentation

Table I. Sample Molecules with Primary Fragmentation Found in the MPRI Mass Spectra

 Adenine I m/e 135	 β -Estradiol II m/e 272
 Tryptamine III m/e 160	 Tryptophan IV m/e 204
 Phenylalanine V m/e 165	 Serotonin VI m/e 176

is presumed to occur since the ejected neutral molecules are found in a variety of excited vibrational and rotational states so that two-photon absorption leaves the ionized molecule with various degrees of excess internal energy. Even with this difficulty, however, detection limits utilizing characteristic fragment ions are equal to or greater than those for SIMS.

EXPERIMENTAL SECTION

The basic experimental apparatus has been described elsewhere (2, 3). Briefly, the vacuum chamber consists of an ion-pumped Perkin-Elmer Ultek TNB-X chamber with a base pressure of 5×10^{-9} Torr. The system is equipped with a load-lock assembly pumped by a Balzers TSU170 170 L/s turbomolecular pump. This assembly allows new samples to be inserted in less than 10 min. A schematic diagram illustrating the arrangement of the important components is shown elsewhere (4).

During the experiment, a 5.6- μ s pulse of primary Ar^+ ions (34 μ A, 10 keV) is generated by a Physicon Model DP10-01 duoplasmatron source. The primary ion beam has a spot diameter of 1 mm and is incident on the target at an angle of 45°. The laser system consists of a Quanta-Ray Model PDL-2 dye laser pumped by a Quanta-Ray Model DCR-2A Nd:YAG laser triggered at a 30-Hz repetition rate. Frequency doubling of the dye laser output is accomplished by using a Quanta-Ray Model WEX-1 wavelength extension unit. Laser energy is monitored by using a Scientech Model 362 power meter.

The biomolecules investigated in this work are shown in Table I. For molecules III, IV, and VI, ionization is initiated by using 280-nm (4.407-eV) radiation based on the absorption characteristics of the indole chromophore (8). The 280-nm radiation is produced from Exciton Rhodamine 590 dye in CH_3OH , yielding up to 5.8 mJ/6 ns (9.7×10^6 W) after frequency doubling. For molecules I, II, and V, ionization is accomplished by using 266-nm (4.639-eV) radiation. This particular wavelength is selected on the basis of the absorption features of the aromatic centers for these compounds and is generated by employing the fourth harmonic of the Nd:YAG laser, yielding up to 3.4 mJ/6 ns (5.7×10^6 W). For experiments requiring less energetic photons, 303-nm (4.073-eV) light is employed for ionization. The 303-nm

radiation is produced from Exciton Rhodamine 640 in CH_3OH , yielding 2.2 mJ/6 ns (3.7×10^6 W) after frequency doubling. The cross-sectional areas of the unfocused 280-, 266-, and 303-nm laser beams are 0.38, 0.49, and 0.39 cm^2 , yielding respective power densities of 2.6×10^6 , 1.2×10^6 , and 9.4×10^6 W/ cm^2 .

Following resonant postionization, the photoions are extracted into a reflecting TOF mass spectrometer and are detected by a Galileo Electro-Optics Corp. Model FTD 2002 dual microchannel plate (MCP) assembly. The resolution of the mass spectrometer varies depending on various parameters, such as laser beam diameter, but it is approximately 100 in the experiments presented here. Time-of-flight mass spectra are recorded by routing the analog signal from the MCP to a 100-MHz Digital Signal Processing (DSP) Technology Model 2001AS transient recorder equipped with a DSP Model 4100 averaging memory and averaging over 1024 laser pulses (34 s). This procedure requires a total dose of 10^{12} incident ions into a 1-mm area. Analog signals are digitized with 8-bit precision by using the transient recorder and are transferred to a Digital Equipment Corporation MicroVaxII by a CAMAC interface. The details of the pulsing/timing sequence used in the experiment have been previously reported (3).

The main source of background is secondary ions that arrive at the detector during an analysis. The intensity of these ions is generally less than 1% of the base peak signal amplitude in the TOF spectra and is typically found only at low masses. The biomolecules studied in this work have negligible vapor pressures at room temperature. Due to the sensitivity of our technique, however, a small gas-phase signal is frequently observed in the absence of any ion bombardment due to vacuum sublimation of the molecular film. This signal usually comprises <1% of the total ion desorbed peak amplitude. Consequently, this gas-phase spectrum, obtained by turning off the incident ion pulse while leaving the MPRI laser on, is subtracted from each wave form.

Samples were deposited onto a silicon substrate that was ultrasonically cleaned in ethanol and mounted on a copper backplate. Silicon was found to yield the lowest background signal compared to other substrates such as Ag, In, or Au. Molecules II-VI were dissolved in analytical-grade water at pH 6.3 to prepare a 10^{-4} M stock solution. A 10- μ L aliquot was then deposited onto the surface of a clean Si wafer. The solvent was removed under high vacuum conditions ($\sim 10^{-6}$ Torr), producing a visually uniform film. For β -estradiol, the solvent of choice was analytical-grade chloroform. The deposition procedure was identical with that for molecules II-VI except that the chloroform solvent was air evaporated. The amount of each biomolecule in the area probed by the ion beam was estimated to be 4×10^{-11} mol. For quantitative studies, a series of standards ranging in concentration from 10^{-7} to 10^{-5} M serotonin in HPLC-grade water was prepared by analytical dilution of a 10^{-3} M stock solution. For each sample, a 10- μ L aliquot was deposited onto the surface a Si substrate. Following vacuum evaporation of the solvent, the sample was inserted into the analysis chamber via a load-lock assembly and analyzed. This procedure was repeated three to four times per analyte concentration, providing independent analyses for each data point. The biomolecules studied were obtained from Sigma Chemical Co. and were used without further purification.

Our reflectron analyzer is capable of recording a TOF SIMS spectrum of each target molecule by appropriate adjustment of the pulse timing, lens, and reflector potentials (4). On Si targets, the SIMS signal was more than 3 orders of magnitude smaller than the MPRI-induced neutral signal and was, in most cases, well into the background noise. In some cases, the SIMS signal could be observed when the samples were placed on Au or Ag targets but with considerably less sensitivity than is observed when using the scheme considered in this work.

RESULTS AND DISCUSSION

We begin with a study of the first two molecules shown in Table I, adenine and β -estradiol. Adenine is interesting since its skeletal backbone contains several heteroatoms, while β -estradiol is markedly less conjugated than the PAC's studied previously. Neither of these molecules possess side chains.

The TOF MPRI spectrum of $\sim 10^{-11}$ mol of adenine desorbed from a silicon surface is shown in Figure 1 using an ionization wavelength of 266 nm. Adenine is a primary con-

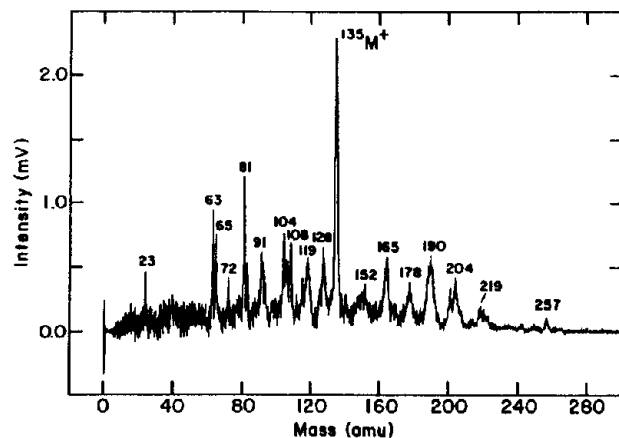


Figure 1. MPRI mass spectrum of $\sim 10^{-11}$ mol of adenine molecules desorbed from the surface of a silicon substrate. MPRI was accomplished by using 266-nm laser radiation at a power density of 1.0×10^6 W/cm².

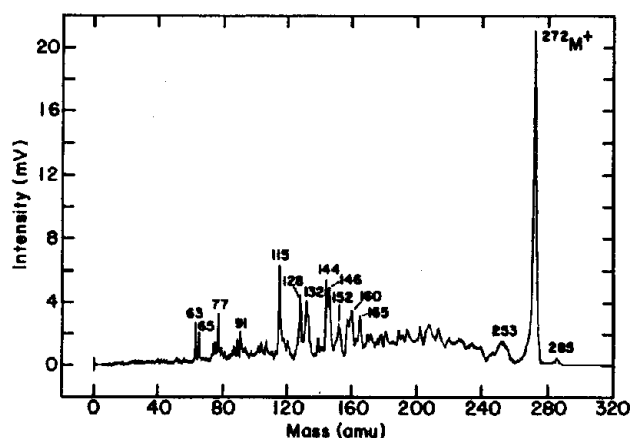


Figure 2. MPRI mass spectrum of $\sim 10^{-11}$ mol of β -estradiol molecules desorbed from the surface of a silicon wafer. MPRI was accomplished by using 266-nm laser radiation at a power density of 1.0×10^6 W/cm².

stituent of nucleic acids and coenzymes that are used in research programs involving heredity, viral diseases, and cancer (9). The salient feature of the spectrum is an intense base peak at 135 amu corresponding to the molecular ion. Other noteworthy fragments are observed at $(M - 16)^+$, $(M - 27)^+$, and $(M - 44)^+$ due to the expulsion of NH_2 , HCN, and H_2NCN (or $\text{NH}_3 + \text{HCN}$). A peak is also visible at m/e 81 ($M - 54$)⁺ due to a loss of two HCN molecules. The signals occurring above m/e 135 may represent sample impurities or possibly several ion-beam-induced reaction products that are unidentified. The molecular ion is also the base peak in the EI mass spectrum of adenine (8). The MPRI spectrum is also very similar to those reported for the ionization of adenine using 266-nm radiation after laser desorption with (10) and without (11) supersonic jet entrainment. A molecule possessing this type of structure is straightforward to characterize by using the MPRI approach. Quantitative studies should be significantly improved over SIMS or FAB experiments where matrix effects can distort measurement reliability.

Similar high-quality spectra have been obtained by using β -estradiol. The MPRI TOF mass spectrum of $\sim 10^{-11}$ mol of β -estradiol, a potent mammalian estrogenic hormone (9), desorbed from the surface of a silicon wafer is presented in Figure 2. The laser was tuned to 266 nm at a power density of 1.0×10^6 W/cm². An intense base signal corresponding to the molecular ion is observed at m/e 272. Also, significant fragmentation of the steroid backbone structure is clearly visible at masses below m/e 260. Very similar results are

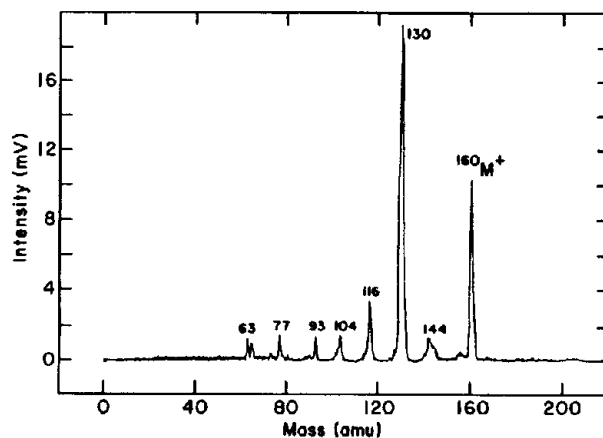


Figure 3. MPRI mass spectrum of $\sim 10^{-11}$ mol of tryptamine molecules desorbed from the surface of a silicon substrate. MPRI was accomplished by using 280-nm laser radiation at a power density of 1.8×10^6 W/cm².

obtained by using EI ionization (8) and laser desorption/MPRI using 266-nm radiation with no supersonic jet cooling (11). This molecule exhibits ideal behavior for our experimental technique.

The next challenge is to determine if our surface characterization approach can be applied to more fragile molecules such as those that possess amino acid side chains. For this study, we have chosen three indolic moieties that possess amine or amino acid functionality. The fourth compound is a simple aromatic amino acid. It is important to note that the skeletal structure for these molecules is significantly more vulnerable to fragmentation than that of a polycyclic aromatic hydrocarbon.

The first molecule studied in this section is tryptamine. Tryptamine is a compound whose CH_2O^- and OH^- derivatives have been shown to exhibit biogenic activity, including neurotransmission (12). The TOF mass spectrum obtained by MPRI detection of $\sim 10^{-11}$ mol of tryptamine desorbed from the surface of a silicon substrate is shown in Figure 3. In this case, photoionization was achieved by using 280-nm radiation at a power density of 1.8×10^6 W/cm². The tryptamine molecular ion signal at m/e 160 is clearly visible, although significant fragmentation is seen in the spectrum. The M^+ signal is present at $\sim 53\%$ abundance relative to the base peak at m/e 130. This signal at $(M - 30)^+$ is due to $\text{C}_\alpha\text{-C}_\beta$ cleavage of the alkylamine side chain. Also observed is a peak at m/e 144 due to loss of an NH_2 radical as well as a signal at $(M - 44)^+$ from complete scission of the side chain. A peak possibly arising from a ring opening of the indole moiety is present at $(M - 56)^+$. In addition, intensities at m/e 93 and 77 are observed, corresponding to C_7H_9^+ and C_6H_5^+ species, respectively.

It is of interest to determine if the molecular fragmentation occurs during the ion desorption event or during the photoionization step. Although we have not tested a wide variety of laser wavelengths and power densities, it is possible to compare our data to other ionization approaches. The electron impact (EI) mass spectrum is very similar to the spectrum shown in Figure 3 (8). In particular, the base signal in the EI mass spectrum of tryptamine occurs at m/e 130, similar to the MPRI results. A small M^+ peak is also observed in the EI spectrum at an abundance of $\sim 22\%$ relative to the base intensity. However, for MPRI of tryptamine following entrainment in a supersonic jet by a high-pressure liquid injection method, different results are obtained (13). In particular, the base peak in the mass spectrum corresponds to the tryptamine molecular ion for an ionization wavelength of 280 nm. This wavelength is very close to the (0-0) excitation

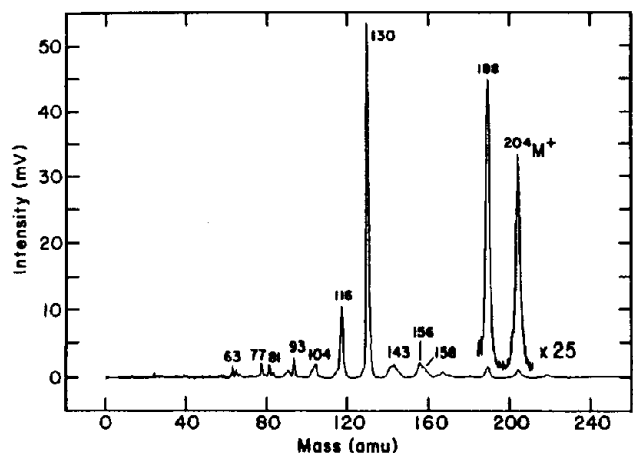


Figure 4. MPRI mass spectrum of $\sim 10^{-11}$ mol of tryptophan molecules desorbed from the surface of a silicon wafer. MPRI was accomplished by using 280-nm laser radiation at a power density of 1.7×10^6 W/cm 2 .

resonance. The m/e 130 fragment is also present but at a low abundance ($\sim 15\%$). When the ionization wavelength is changed to 266 nm, the m/e 130 fragment abundance increases to $\sim 54\%$ (13). Similar observations are found using 266-nm photons after laser desorption into a supersonic jet (14).

It is straightforward to understand these observations, at least in a qualitative fashion. The enhanced fragmentation at 266 nm presumably is observed since absorption of the second photon produces a molecular ion in a higher energy excited state. This state may then decay by fragmentation. Laser power densities do not become important from a fragmentation point of view until there are a significant number of molecules absorbing photons in excess of those needed for ionization. Typical MPI conditions are in this range, resulting in hard ionization due to the excess energy imparted to the molecules by the extra photons absorbed. The photoionization spectrum for jet-cooled tryptamine at 266 nm is similar to the EI spectrum since electron impact also leaves the molecular ion in a high-energy excited state. The spectrum shown in Figure 3 exhibits fragmentation since the initial state of the molecule consists of a broad range of vibrational and rotational excited states due to the desorption step. After absorption from excited vibrational levels, a broad range of molecular ion states will be produced, some of which will lead to fragmentation. It is interesting to note that for all of the molecules studied changing the primary beam energy between 6 and 10 keV did not affect the degrees of fragmentation observed. This is not unexpected since the desorbing molecules typically see only a few electronvolts of the primary ion's energy (15). These data all suggest, then, that the photodissociation process and not the ion beam desorption process is the primary process that creates the fragment ions.

Very similar trends are observed for tryptophan, a closely related amino acid. This molecule serves as a precursor to a variety of biogenic indoles (12). Moreover, it is a common constituent of many peptides. As such, this molecule can serve as an absorbing center for the MPRI analysis of peptides and proteins. The TOF mass spectrum of $\sim 10^{-11}$ mol of tryptophan desorbed from the surface of a silicon substrate is shown in Figure 4. When ionized by using 280-nm radiation at a power density of 1.7×10^6 W/cm 2 , the base peak is again found at m/e 130 and corresponds to $C_\alpha-C_\beta$ cleavage of the amino acid side chain. In this case, the M^+ signal intensity is of very low abundance ($\sim 3\%$). Also, peaks at $(M - 16)^+$, $(M - 46)^+$, and $(M - 61)^+$ are observed for structure-specific losses of NH_2 and $HCOOH$ and the simultaneous loss of both the NH_2 and $COOH$ radicals, respectively. A peak possibly arising from a ring-opening reaction of the indole unit is visible

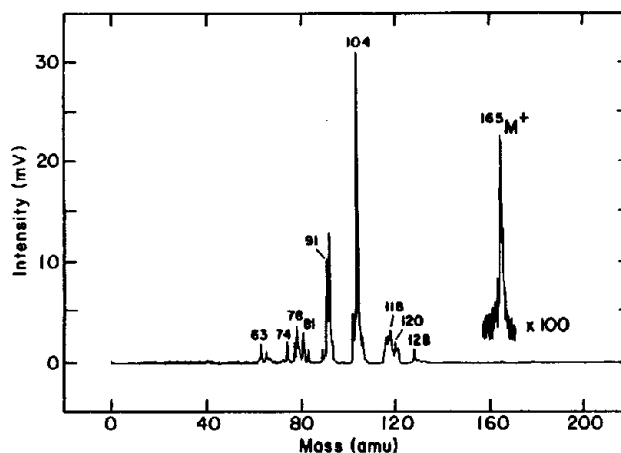


Figure 5. MPRI mass spectrum of $\sim 10^{-11}$ mol of phenylalanine molecules desorbed from the surface of silicon. MPRI was accomplished by using 266-nm laser radiation at a power density of 1.0×10^6 W/cm 2 .

at $(M - 100)^+$, similar to the tryptamine case. A reasonably intense signal at $(M - 88)^+$ is seen due to complete loss of the amino acid side chain. As for tryptamine, the EI spectrum exhibits a base peak at m/e 130 and a very small M^+ signal at m/e 204 in low abundance ($\sim 5\%$) (8). In contrast, the molecular ion of tryptophan is the base peak in the mass spectrum for MPRI using 286-nm photons after laser desorption into a supersonic jet (16). For an ionization wavelength of 266 nm, the fragment ion at m/e 130 is the base peak in the mass spectrum and the relative abundance of the M^+ signal decreases to 40% (16).

For this molecule, it is possible to compare the photoionization spectra to the fast atom bombardment (FAB) spectrum. With FAB, the base peak is observed at m/e 205, which corresponds to MH^+ (17). The biggest fragment peak is found at m/e 130 but is observed at a low intensity (33%). Ionization that occurs during the bombardment event yields the lowest level of fragmentation of all of the methods noted above. This observation again strongly suggests that MPRI of vibrationally excited molecules can lead to photodissociation, presumably due to the formation of a variety of excited molecular ion states.

The MPRI TOF mass spectrum of $\sim 10^{-11}$ mol of phenylalanine desorbed from a silicon surface is shown in Figure 5. This molecule is a typical constituent of peptides and proteins and, like tryptophan, can be used as an absorbing center for peptide sequencing. The laser was tuned to 266 nm and operated at a power density of 1.0×10^6 W/cm 2 . A weak M^+ signal is observed at m/e 165, which is roughly 150-fold lower in intensity than the base peak. The base signal at m/e 104 corresponds to phenylalanine radical loss of $COOH$ and NH_2 . Also observed at 120 amu is a peak due to M^+ elimination of $COOH$. An intense $(M - 74)^+$ signal shows efficient $C_\alpha-C_\beta$ cleavage of the amino acid chain. This is in contrast to the EI spectrum of phenylalanine where the base peak occurs at 120 amu (8). However, both the EI and MPRI spectra show very low M^+ abundance. Contrary to the MPRI and EI data, the molecular ion of phenylalanine is the base signal in the laser desorption mass spectrum using 266-nm MPRI after supersonic beam entrainment (16) and in the FAB spectrum.

We have examined the implications of fragmentation induced by the MPRI process relative to the problem of trace organic surface analysis. Our model system is serotonin, a potent neurotransmitter that has been shown to influence appetite, memory, sexual drive, and depression. The MPRI mass spectrum of $\sim 10^{-11}$ mol of serotonin desorbed from a silicon surface is shown in Figure 6a using 1.9×10^6 W/cm 2 of 280-nm radiation. As observed for the previous molecules,

Table II. MPRI Experimental Data for Serotonin Standards on Silicon

mol sampled	av intensity, mV ^a	no. of incident ions ^b	laser peak power, W	normalized intensity ^c
4.11×10^{-12}	25.48 ± 1.16	1.2×10^{12}	5.7×10^6	7.25 ± 0.33
2.05×10^{-13}	9.76 ± 0.76	1.2×10^{12}	5.9×10^6	2.69 ± 0.21
4.11×10^{-13}	2.83 ± 0.20	1.2×10^{12}	5.9×10^6	0.783 ± 0.056
2.05×10^{-13}	1.23 ± 0.092	1.2×10^{12}	6.3×10^6	0.319 ± 0.024
4.11×10^{-14}	0.37 ± 0.16	1.3×10^{12}	5.9×10^6	0.092 ± 0.039

^a Actual signal intensity averaged over four independent replicates. ^b Average ion dose measured by using a 6- μ s ion pulse with a peak current of approximately 34 μ A and a 30-Hz repetition rate. ^c Obtained by averaging the signal intensities that have been normalized to account for ion current and laser power variations between individual runs.

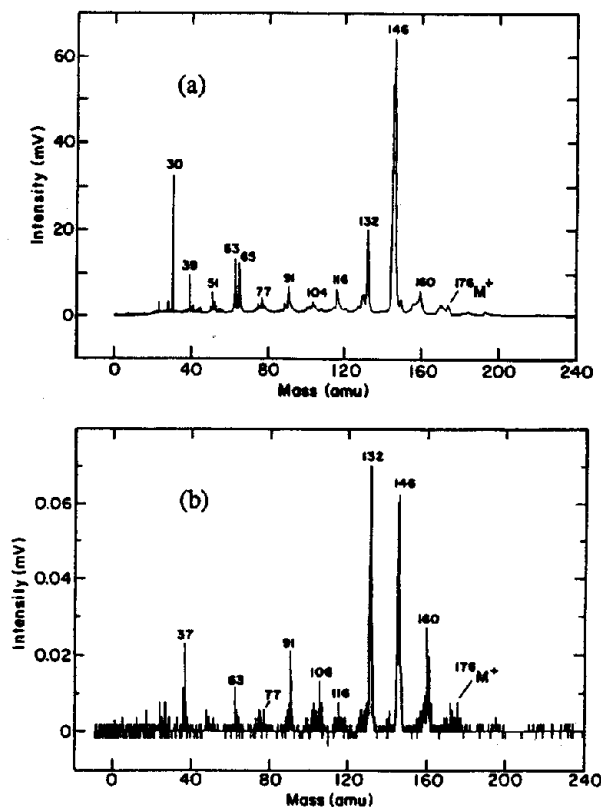


Figure 6. (a) MPRI mass spectrum of $\sim 10^{-11}$ mol of serotonin molecules ion beam desorbed from a silicon surface. (b) MPRI gas-phase mass spectrum of a thick film of serotonin molecules. The number of gas-phase molecules present in the ionization volume is estimated to be 10^4 – 10^5 . In both cases, MPRI was accomplished by using 280-nm laser radiation and operated at a power density of 1.9×10^6 W/cm².

the base peak in the spectrum corresponds to a fragment ion arising from the C_α–C_β cleavage of the alkylamine side chain at (M – 30)⁺. The signals at (M – 16)⁺ and (M – 44)⁺ are easily assigned to radical loss of NH₂ and complete removal of the amine side chain. A weak M⁺ signal at *m/e* 176 is present at a low abundance of $\sim 4\%$. The peak at *m/e* 104 is also observed for tryptamine and tryptophan. As is the case for the other amines, the EI spectrum is quite similar (8). The *m/e* 146 fragment is the base peak in agreement with the MPRI results, although the M⁺ ion abundance is ~ 6 -fold higher at $\sim 24\%$. The MPRI spectra are again similar to those reported for the MPRI of serotonin using 266-nm radiation after laser desorption into a supersonic jet (13). Upon cooling, the molecular ion signal and the *m/e* 146 fragment ion are present at an equal abundance of 100%.

The serotonin molecule is interesting in that a small MPRI signal is observed with the ion beam switch off. This signal arises from sublimation of serotonin from the target. The spectrum of this vapor is shown for comparison purposes in Figure 6b. Note that the fragmentation pattern is very similar

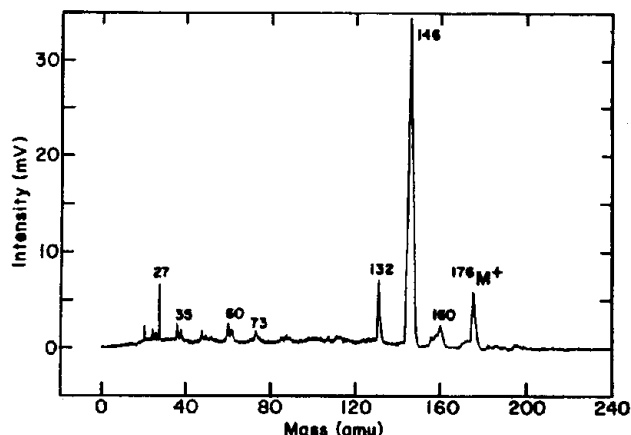


Figure 7. MPRI mass spectrum of $\sim 10^{-11}$ mol of serotonin molecules desorbed from a silicon surface. MPRI was accomplished by using 303-nm laser radiation and operated at a power density of 8.3×10^6 W/cm².

to that found for the serotonin desorbed by the ion beam. These results provide the strongest evidence yet that fragmentation is dominated by the laser ionization step and *not* by the ion beam desorption step.

To develop analytical procedures for trace analysis, it is desirable to lock onto a structurally significant ion peak of the largest possible intensity by using the most selective laser ionization scheme. We have not exhaustively examined all excitation possibilities for serotonin but have attempted to photoionize using 303-nm radiation as seen in Figure 7. This wavelength does not exceed the threshold for (0–0) band excitation at 286 nm, so any ionization should occur from excited vibrational levels. The results, shown in Figure 6b, indicate that for excitation at 8.3×10^6 W/cm² of 303-nm radiation that the M⁺ ion signal is larger than that found for 280-nm radiation. Moreover, when adjusted for the laser power difference, the *m/e* 146 peak is of comparable intensity. For these experiments, then, either wavelength would be suitable for trace analytical studies. These interesting observations suggest that additional experiments that exploit still other ionization schemes may lead to improved soft ionization processes.

In order to provide an estimate of the sensitivity of the MPRI method, a set of serotonin standards were prepared by analytical dilution. Specifically, 1×10^{-12} – 1×10^{-10} mol of serotonin was deposited into a 0.2-cm² area on a silicon substrate. During these analyses, the incident ions were focused into a 0.008-cm² beam spot. Consequently, only $\sim 4\%$ of the total available analyte surface area was probed by the ion beam during the experiments. Therefore, the calculated amount of serotonin in the ion beam sampling area ranged from 40 fmol to 4 pmol. The amplitudes of the serotonin *m/e* 146 base peaks at different concentrations were measured and individually normalized to the experimental laser power and ion current values. The results are presented in Table II. A

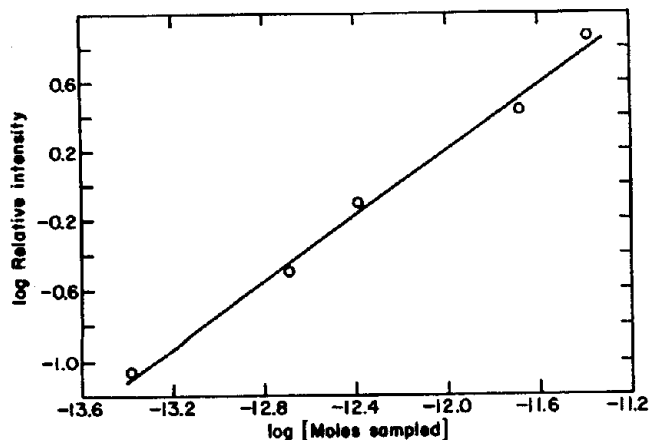


Figure 8. MPRI intensity of the serotonin 146 amu base peak versus the concentration of serotonin in the ion beam sampling area. See Table II for additional information.

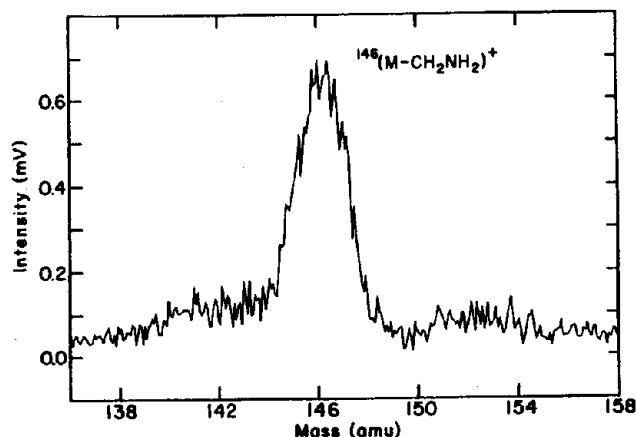


Figure 9. Portion of the MPRI mass spectrum for a 40-fmol serotonin target in the base peak region. The laser was tuned to 280 nm and operated at a power density of $\sim 10^8$ W/cm².

plot of relative signal intensity versus sample concentration is shown in Figure 8. Although the data are presented in logarithmic form, the slope of the normalized linear plot is 0.969 ± 0.031 . The base peak region in the TOF mass spectrum of a typical 40-fmol target is shown in Figure 9. Note that the base signal is clearly visible above the noise at this low level of analyte concentration. A detection limit is calculated by determining the signal-to-noise (S/N) ratio for each of four independent 40-fmol analyses and extrapolating to a S/N level of 2. When the adjusted concentrations are further scaled to reflect an achievable incident ion current of 100 μ A, a detection limit of 5×10^{-16} mol of analyte present in the area probed by the ion beam is obtained.

This limit corresponds to the detection of 3×10^9 molecules or 4×10^{-8} monolayers using the assumption that a 1 monolayer coverage contains 1×10^{14} molecules spread over 1 cm². These measurements are significant since they yield extremely low detection limits even though the molecular ion exhibits considerable photodissociation. We believe these limits can be pushed at least 2 orders of magnitude lower with a number of simple steps. First, recent imaging experiments suggest uniform sample deposition is extremely difficult using our deposition techniques. The deposited film can spread unevenly over the sample and may form small crystallites. New methods of preparing surfaces with trace levels of organic molecules will be an important future area for research. Target cooling to prevent loss of sample by sublimation may also be necessary. Second, we have recorded our ion signal using only very low ion doses. Recently, it has been observed that significant signals persist during depth profiling (18). If this

observation proves generally correct, it may be possible to increase the sampling volume and reduce the detection limit in samples where surface sensitivity is not of importance. Third, we have addressed the issues associated with laser power and wavelength in only a preliminary fashion. It is anticipated that we are far from finding the optimal laser schemes. Finally, it can be noted from Figure 6 that considerable intensity with structural specificity exists at other masses. It will certainly be feasible to improve detection limits further by including all of these signals in our analysis.

CONCLUSIONS

During the last decade, we have certainly seen dramatic changes in the approach to characterizing thermally labile organic molecules in the solid state. A range of techniques now allow molecules with a wide range of molecular weights to be detected in a variety of matrices by mass spectrometry. Our work has focused on the use of ion-beam-induced desorption followed by MPRI of the desorbed neutral molecules. This scheme offers significant advantages for a particular class of experimental configurations. For example, ion beams desorb molecules only from the first few layers of the solid, making them a surface-sensitive probe (19). The MPRI detection scheme is especially appropriate for several reasons. These include the fact that for many experimental situations, since the neutral flux greatly exceeds the ion flux, a more quantitative measure is possible than with competing techniques such as SIMS, and detection of extremely low levels of surface organic impurities is feasible.

In this work, we have shown that MPRI is a relatively soft ionization technique as compared to electron beam multiphoton ionization that performs its function with high efficiency. It yields molecular ions for many systems even without using jet cooling to rid the molecules of excess vibrational energy. For more fragile molecules with sidechains, it is still possible to produce structurally significant fragment ions that are detectable at the femtomole level and probably below. More sophisticated laser schemes may provide even softer ionization than is observed here. In general, we believe that the prototypical results presented here open many new experimental directions for the detection of biomolecules. We are particularly interested in taking advantage of the limited selectivity of MPRI and the high selectivity of mass spectrometry to detect these molecules in more complex matrices. We expect, for example, that special matrices that enhance ionization such as glycerol will not be needed. Finally, the sensitivity limits demonstrated in this work suggest that this approach will not only be valuable for trace organic surface analysis but also for molecular imaging. For imaging experiments, the number of available molecules is less than $10^4/\mu^2$.

Registry No. Adenine, 73-24-5; β -estradiol, 50-28-2; tryptamine, 61-54-1; tryptophan, 73-22-3; phenylalanine, 63-91-2; serotonin, 50-67-9.

LITERATURE CITED

- (1) Winograd, N.; Baxter, J. P.; Kimock, F. M. *Chem. Phys. Lett.* **1982**, *88*, 581-584.
- (2) Kimock, F. M.; Baxter, J. P.; Pappas, D. L.; Kobrin, P. H.; Winograd, N. *Anal. Chem.* **1984**, *56*, 2782-2791.
- (3) Pappas, D. L.; Hrubowchak, D. M.; Ervin, M. H.; Winograd, N. *Science* **1989**, *243*, 64-66.
- (4) Hrubowchak, D. M.; Ervin, M. H.; Winograd, N. *Anal. Chem.* **1991**, *63*, 225-232.
- (5) Pollin, M. H.; Young, C. E.; Calaway, W. F.; Burnett, J. W.; Jorgensen, B.; Schweltzer, E. L.; Gruen, D. M. *Nucl. Instrum. Meth. Phys. Res.* **1987**, *B18*, 446-451.
- (6) Parks, J. E.; Schmitt, H. W.; Hurst, G. S.; Fairbank, W. M., Jr. *Thin Solid Films* **1983**, *108*, 69-78.
- (7) Grottemeyer, J.; Schlag, E. W. *Org. Mass. Spectrom.* **1988**, *23*, 388-396.
- (8) McLafferty, F. W.; Stauffer, D. B. *The Wiley/NBS Registry of Mass Spectral Data*; John Wiley and Sons, Ltd.: New York, 1989; Vols. 1-3.
- (9) *The Merck Index*, 11th ed.; Budavari, S., Ed.; Merck and Co., Inc.: Rahway, NJ, 1989.

- (10) Li, L.; Lubman, D. M. *Int. J. Mass Spectrom. Ion Proc.* **1989**, *88*, 197-210.
- (11) Hahn, J. H.; Zenobi, R.; Zare, R. N. *J. Am. Chem. Soc.* **1987**, *109*, 2842-2843.
- (12) Hooper, R. J. L. In *Recent Developments in Mass Spectrometry in Biochemistry, Medicine, and Environmental Research 7*; Frigerio, A., Ed., Elsevier Scientific Publishing Company: Amsterdam, 1981; pp 69-84.
- (13) Pang, M.; Sin, C. H.; Lubman, D. M. *Appl. Spectrosc.* **1988**, *42*, 1200-1206.
- (14) Li, L.; Lubman, D. M. *Anal. Chem.* **1989**, *61*, 1911-1915.
- (15) Garrison, B. J. *Int. J. Mass Spectrom. Ion Phys.* **1983**, *53*, 243-254.
- (16) Grottemeyer, J.; Walter, K.; Boesl, U.; Schlag, E. W. *Int. J. Mass Spectrom. Ion Proc.* **1987**, *78*, 69-83.
- (17) Kulk, W.; Heerma, W. *Biomed. Environ. Mass Spectrom.* **1988**, *15*, 419-427.
- (18) Gillen, G.; Simons, D. S.; Williams, P. *Anal. Chem.* **1990**, *62*, 2122-2130.
- (19) Harrison, D. E., Jr.; Kelly, P. W.; Garrison, B. J.; Winograd, N. *Surf. Sci.* **1978**, *78*, 311-322.

RECEIVED for review March 7, 1991. Accepted June 10, 1991.
We are grateful to the National Science Foundation, the Office of Naval Research, the Department of Energy, and IBM Corp. for financial support of this work.